Phytoplankton and seston fatty acid dynamics in the northern Bering-Chukchi Sea region

Jens M. Nielsen[a,b,*], Louise A. Copeman[c,d,e], Lisa B. Eisner[a], Kelia E. Axler[a], Calvin W. Mordy[b,f] Michael W. Lomas[g]

[a]*NOAA Alaska Fisheries Science Center, 7600 Sand Point Way NE, Seattle, WA, 98115, USA*
[b]*Cooperative Institute for Climate, Ocean, and Ecosystem Studies, University of Washington, Seattle, WA, United States*
[c]*NOAA Alaska Fisheries Science Center, 2030 SE Marine Science Dr., Hatfield Marine Science Center, Newport, OR, 97365, USA*
[d]*College of Earth, Ocean, and Atmospheric Sciences, Oregon State University, 104 CEOAS Administration Building, Corvallis, OR, 97331, USA*
[e]*Cooperative Institute for Marine Ecosystem and Resources Studies, Oregon State University, 2030 SE Marine Science Drive, Newport, OR, 97365, USA*
[f]*NOAA Pacific Marine Environmental Laboratory, Seattle, WA, USA*
[g]*Bigelow Laboratory for Ocean Sciences, 60 Bigelow Dr., East Boothbay, ME, 04544, USA*

*Corresponding author.
E-mail address: jens.nielsen@noaa.gov (J.M. Nielsen)

KEYWORDS: Fatty acids, Arctic, Chukchi Sea, Northern Bering Sea, Phytoplankton

ABSTRACT

Arctic and subarctic ecosystems are transitioning due to ocean warming, resulting in conditions that will lead to shifts in phytoplankton communities, their nutritional compositions, and production of fatty acids (FAs). FA biomarkers are useful indicators of changing phytoplankton

community composition and provide insight into basal resource quality for higher trophic level consumers such as zooplankton, fish, birds and marine mammals, yet phytoplankton FA information is largely lacking from the Bering and Chukchi Sea regions. Therefore, we analyzed suspended particulate matter (seston) FAs, chlorophyll-a (Chl-a) and environmental data collected from four surveys in the North Bering and Chukchi Seas, two during June of 2017 and 2018 and two during August and September 2017 and 2019. Our objectives were to determine 1) whether seston FA composition was correlated with phytoplankton taxonomic composition analyzed using imaging microscope (FlowCAM) techniques, 2) if there were seasonal differences in seston FA concentrations, and 3) how FA concentrations vary with environmental variables. We found significant seasonal differences in seston FA compositions, with diatom biomarkers more prevalent in spring, followed by a community shift to dinoflagellate and small flagellate FA biomarkers in late summer. These results were confirmed by FlowCAM analyses. FA biomarkers were correlated with total and large size-fractioned Chl-a concentrations, nitrogen concentration and temperature. Lastly, we used a model framework to predict availability of the diatom-associated essential FA, eicosapentaenoic acid (EPA, 20:5n-3). Our analysis provides new information on phytoplankton FA dynamics and the important nutritional role of phytoplankton for higher trophic level consumers in the northern Bering and Chukchi Sea regions.

1. Introduction

The Bering and Chukchi seas are some of the most productive areas of the Arctic Ocean (Hill et al., 2018). A pronounced diatom spring bloom commonly associated with the timing of ice breakup (Fujiwara et al., 2016; Laney and Sosik, 2014) fuels pelagic and benthic secondary production (Grebmeier et al., 2006; Sigler et al., 2014). Later in the season, once the ocean stratifies, a majority of the large size-fractioned phytoplankton biomass is often present in subsurface waters (Martini et al., 2016) while smaller sized plankton occur in the surface waters (Giesbrecht et al., 2019). Due to ocean warming, Arctic and subarctic marine ecosystems, including the Bering and Chukchi Seas, are undergoing rapid changes in their physical and thus biological function (Huntington et al., 2020). Projected changes in the coming decades include changing sea-ice phenology, spring bloom timing and phytoplankton production (Clement Kinney et al., 2020; Hermann et al., 2019; Song et al., 2021). These changes also influence the production of fatty acids (FAs) synthesized by phytoplankton which play an essential nutritional role for the growth and functioning of marine consumers (Copeman et al., 2022; Kainz et al., 2004). More baseline data on phytoplankton nutrition, including their FA compositions is needed for tracking potential short and long-term changes in the quality of basal resources in the Bering and Chukchi Sea food webs.

Phytoplankton play a fundamental nutritional role in marine ecosystems due to their ability to synthesize dietary FAs required by higher trophic level organisms (Budge et al., 2014; Dalsgaard et al., 2003). Marine consumers generally lack the ability to synthesize several essential FAs at a sufficient rate to meet their metabolic demand (Helenius et al., 2020), and therefore require FAs preformed in their diets (Bell and Tocher, 2009). Several essential polyunsaturated FAs (PUFAs), including eicosapentaenoic acid (EPA, 20:5n3) and docosahexaenoic acid, (DHA, 22:6n3), are central compounds that regulate cell membrane

fluidity, neurological functioning, hormones and growth (Bell and Tocher, 2009; Helenius et al., 2019; Tocher et al., 2019). Dietary limitation of essential PUFAs directly influence zooplankton fecundity and growth rates (Leiknes et al., 2016; Pond et al., 1996), survival of larval (Copeman and Laurel, 2010) and juvenile fishes (Bell et al., 1995), and diminished overall ecosystem productivity (Litzow et al., 2006). Because of the direct link between animal growth rates and FA availability, particularly essential FAs, analyses of FA biomarkers can be useful for categorizing ecosystem scale food quality dynamics (Galloway and Winder, 2015; Litzow et al., 2006). The relative amounts of specific FAs vary among phytoplankton taxa (Cañavate, 2019; Parrish, 2013), thus changes in phytoplankton community compositions induce shifts in the dietary FA pool available for consuming organisms (Galloway and Winder, 2015). The association between specific FAs and certain taxonomic groups also make FAs useful biomarkers of phytoplankton compositional changes (Dalsgaard et al., 2003). Yet, the utility of FA biomarkers to partition phytoplankton taxa is known primarily from monoculture experiments (Cañavate, 2019; Dunstan et al., 1993; Jónasdóttir, 2019). Using FA biomarkers to distinguish phytoplankton taxa in field samples is more challenging (Reuss and Poulsen, 2002), variable, and less studied (Galloway and Budge, 2020; Marmillot et al., 2020). Nonetheless, field studies in other high latitude systems, such as the Beaufort Sea (Connelly et al., 2016; Marmillot et al., 2020), West Greenland Sea (Reuss and Poulsen, 2002), and Barents Sea (Falk-Petersen et al., 1998) have highlighted that changes in phytoplankton composition, including seasonal shifts from diatoms to flagellates, are visible in the seston FA pools. Beyond the primary association with a specified phytoplankton taxonomic group, individual FA biomarkers vary with environmental conditions (Sushchik et al., 2004). Shifting environmental conditions influence measured seston FA biomarker concentrations by changing both the individual phytoplankton

FA composition and/or by shuffling the phytoplankton community composition. For example, increasing temperature at the individual species level has been shown to promote increased levels of saturated FAs (SFAs) and monounsaturated FAs (MUFAs), while also decreasing levels of PUFAs (Jiang and Gao, 2004). This decrease in phytoplankton PUFAs with increasing temperature has also been observed in a meta analyses of seston at the community level (Hixson and Arts, 2016). Similarly, nitrogen deficiency have been shown to lower PUFA relative concentrations and increase MUFAs in diatoms (de Jesús-Campos et al., 2020), though different species respond variably to nutrient limitation (Bi et al., 2014). Although biomarker FAs provide valuable information about food quality, they are often not diagnostic or species-specific but should rather be viewed as indicative of dominance from broad taxonomic groups (i.e., predominance of diatoms versus flagellates (Jónasdóttir, 2019), particularly when evaluating field data. Therefore, additional species information from microscopy imaging techniques are beneficial to validate observed FA biomarker patterns (Marmillot et al., 2020).

Here we use FA biomarkers as indicators of changing phytoplankton community compositions, and of basal resource quality for higher trophic level consumers. We analyzed suspended particulate matter (seston) FAs, chlorophyll-a (Chl-a), phytoplankton taxonomic data, and environmental data from four surveys spanning the northern Bering-Chukchi Sea region, two during spring (June) in 2017 and 2018 and two during late summer (August/September) in 2017 and 2019. We examine:

1) Seasonal and annual patterns in both absolute FA concentrations and percent FA composition;

2) the relationship between phytoplankton taxonomic data (dinoflagellates and diatoms) determined from imaging microscope analyses (FlowCAM) compared to specific FA biomarkers;

3) the relationship between individual FA biomarkers and physical, chemical, and biological variables; and

4) show how a simple model framework to predict concentrations of the diatom-sourced essential FA, EPA, can provide a proxy for available basal food quality at a large spatial scale in the northern Bering and Chukchi Sea region, which is an area that currently has very little information on FA biomarker dynamics.

2. Methods

2.1. Data collection

Four surveys were conducted in the northern Bering-Chukchi Sea region as part of the Arctic Integrated Ecosystem Research Program (AIERP, Baker et al., 2020, 2022, https://www.nprb.org/arctic-program), during June of 2017 and 2018 (Arctic Shelf Growth, Advection, Respiration, and Deposition Rate Experiments [ASGARD]) and during August and September (hereafter Aug/Sep) of 2017 and 2019 (Arctic Integrated Ecosystem Survey; Fig. 1). All data are publicly available in the DataONE repository (https://doi.org/10.24431/rw1k5a0). Data included vertical profiles of temperature and salinity were collected from surface to near-bottom at each station using a Sea-Bird Electronics (SBE) 9+ CTD, data processed and averaged

into 1-m bins. Water samples were collected from 5 L (EIS 2017), 10 L (EIS 2019) or 12 L (ASGARD 2017-2018) Niskin bottles attached to the CTD rosette. At every sampling station, total and size-fractioned (<5, 5-20, >20 μm) Chl-a (mg m^{-3}) samples were collected. Total Chl-a samples were collected at 10 m intervals (~5-6 depths) and filtered through 25 mm Whatman GF/F filters (nominal pore size 0.7 μm). Size-fractionated samples were collected at 2-3 depths using a stacked filtration unit, using 47 mm Whatman GF/F filters for <5 μm, and 47 mm polycarbonate filters with a pore size of 5 and 20 μm, to sample the 5-20 and >20 μm large size fractions. Filters were stored frozen (−80 °C) and analyzed within 6 months with a bench top Turner Designs Trilogy fluorometer using standard extraction methods (acidification technique, Parsons, 1984). Samples for dissolved inorganic nutrients (nitrate, nitrite, ammonium, phosphate, and silicic acid; μmol kg^{-1}) were collected from each Niskin bottle, filtered through 0.45 cellulose acetate filters, and frozen. Samples were analyzed on a Seal AA3 or Seal AA500 continuous segmented flow analyzer following methods in (Gordon et al., 1993). Ammonium was analyzed using the OPA method (Holmes et al., 1999). Seston samples for FA analyses were collected at 1-2 depths at every other station (n = 164).

Phytoplankton community samples (pre-screened with 200 μm Nitex mesh) were analyzed for cell abundance using Fluid Imaging Technologies VS Series benchtop FlowCAM (hereafter referred to as FlowCAM) using a 10× objective and 200 μm flow cell in autoimage mode (Álvarez et al., 2014). Particle images with lengths > 20 μm diameters were manually counted from two surveys in June 2017 and Aug/Sep 2017. Images were grouped into diatoms or dinoflagellates. Diatoms were imaged in both June and Aug/Sep 2017, while dinoflagellates were imaged only in Aug/Sep 2017. Biovolumes of cells were estimated from images using the biovolume estimation function (cylindrical shape) in the VisualSpreadsheet (Scarborough, ME)

software provided with the instrument. These estimates compared well with manual estimates of biovolume using standardized shapes and appropriate geometric equations (Menden-Deuer and Lessard, 2000). FlowCAM biovolumes of diatoms and dinoflagellates were compared to concentrations of the FA biomarkers of diatoms and dinoflagellates, and the ratio of DHA: EPA.

2.2. Fatty acid analyses

We collected FA seston samples, which comprise all living and non-living material between 0.7-200 μm, such as phytoplankton, heterotrophic protists, bacteria, mesozooplankton eggs and nauplii, and detritus. Phytoplankton commonly constitute the majority of the seston material (Connelly et al., 2016; Hama, 1999) and thus the majority of the seston FAs can be attributed to FA phytoplankton. Water samples (prescreened through a 200 μm Nitex mesh) ranging in volume from 2 L to 6 L were collected for seston FA analysis on each of the four surveys. Samples were collected from the surface, Chl-a maximum (estimated from the CTD fluorescence down cast data at the time of sampling), or at near-bottom depths. Each bottle was filtered onto a pre-combusted Whatman 47 mm GF/F filter (0.7 μm nominal pore size), and sample filters were stored aboard the ship at -80°C. Samples were shipped frozen on dry ice to the Hatfield Marine Science Center (HMSC) in Newport, Oregon, and analyzed at the Marine Lipid Ecology Laboratory. To obtain sufficient material, some filters were combined for each sampling depth (1-3 filters), placed into lipid-clean glass tubes and stored in chloroform under nitrogen for less than 3 months prior to extraction. Lipids were extracted using a modified Folch procedure (Folch et al., 1957) using 2:1 chloroform: methanol as described by Parrish et al. (1999). A total of 164 seston samples were processed for FA analyses. An internal standard (23:0

methyl ester) was added to all samples at approximately 10% of the total FA concentration, and total lipid extracts were derivatized into their FA methyl esters (FAMEs) using sulphuric acid-catalyzed transesterification (Budge et al., 2006).

Resulting FAMEs were analyzed on an HP 7890 GC FID equipped with an autosampler and a DB wax+ GC column (Agilent Technologies, Inc., U.S.A.). The column was 30 m in length, with an internal diameter of 0.25 mm and film thickness of 0.25 μm. The column temperature began at 65 °C and held this temperature for 0.5 min. Temperature was increased to 195 °C (@ 40 °C min^{-1}), held for 15 min then increased again (@ 2 °C min^{-1}) to a final temperature of 220 °C, where it was held for 1 min. The carrier gas was hydrogen, flowing at a rate of 2 ml min^{-1}. Injector temperature was set at 250 °C and the detector temperature was constant at 250 °C. Peaks on the resulting chromatographs were identified using retention times based upon standards purchased from Supelco (37 component FAME, BAME, PUFA 1, PUFA 3) and in consultation with retention index maps performed under similar chromatographic conditions as our GC-FID (Wasta and Mjøs, 2013). Column function was checked by comparing chromatographic peak areas to empirical response areas using a quantitative FA mixed standard, GLC 487 (NuCheck Prep). Chromatograms were integrated using Chem Station (version A.01.02, Agilent). Select samples were run in triplicate and the coefficient of variation for peaks >1% of the sample, were less than one.

2.3. Statistical analyses

Absolute FA concentrations, the amount of seston FAs per volume seawater (reported as mg m^{-3}), were used to infer overall availability of FAs in the water. FA data were also calculated

as percent mass of total FAs, which is a useful metric for quantifying phytoplankton compositional change. FAs were classified as C:Bn-P, where C is the number of carbon atoms, B the number of double bonds and P the position of the first double bond from the methyl group end (Budge et al., 2006). We considered two aspects of phytoplankton FA composition. Firstly, we focused on phytoplankton biomarkers, such as those indicative of diatoms: 16:1n-7, 16:4n-1, EPA (20:5n-3) and a composite diatom biomarker based on the ratio of 16:1n-7/16:0 (Budge and Parrish, 1998; Dalsgaard et al., 2003). Flagellates are a diverse group, including small autotrophic flagellates, heterotrophic flagellates and dinoflagellates. Therefore, we refer to the biomarkers 18:4n-3, 18:5n-3 and DHA (22:6n-3) as a combination of flagellate and dinoflagellate (dino+flag) FA biomarkers, due to the difficulty in partitioning among these groups using FAs alone. Secondly, we focused on long-chain PUFAs (C_{20+22}) such as EPA and DHA, which are essential in the diet of secondary consumers. In addition, we assessed the ratio of DHA to EPA to denote relative contribution of dino+flag: diatoms and the sum of all odd and branched FA chains as an indicator of bacterial contribution (Kaneda, 1991).

Type II regressions using $\log_{10}$-transformation were used to assess pairwise relationships between FA concentrations, and biological and physical variables including temperature, salinity, nutrients, and total and size-fractioned Chl-a concentrations. One-way Analysis of Variance (ANOVA) with associated post-hoc Tukey Honestly Significant Difference (HSD) was used for group comparisons, such as between seasons, years, depth category (above, below or in the mixed layer) and water mass designations (warm shelf water, cool shelf water, Anadyr water, modified winter water, and warm coastal water, Danielson et al., 2020). ANOVA models were assessed for normality and homogeneity of variances of the residuals and variables were $\log_{10}$-transformed when necessary. Non-metric multidimensional scaling (nMDS) using Bray-Curtis

distances was used to assess multivariate patterns of the FA percent data, using all FAs that constituted more than 1% of the total FAs, and the groups SFA, MUFA, PUFA and Bacterial FAs.

2.4. Model analyses

Linear mixed effects models (Zuur et al., 2009) were used to assess how multiple physical and biological parameters influence the FA composition of seston samples, and then to develop a simple model framework that allows prediction of water column (0-50 m) integrated EPA (mg m^{-2}) concentrations over broader spatial or temporal scales. For each FA biomarker the initial full linear mixed effects model included the following predictor variables: total Chl-a, temperature, nitrogen (sum of nitrate and ammonium), salinity and depth (a categorical variable as described earlier), because these variables have previously been shown to influence the FA composition of phytoplankton (Budge et al., 2014; Galloway and Winder, 2015). The different surveys were included as a random effect because the relationships between FAs and environmental variables could likely be independent among years and season. For all models, inspections of residual plots did not reveal obvious deviances from normality or homoscedasticity after log-transformation of variables. In cases of multicollinearity (variance inflation factor (VIF) > 5), we retained only one of those values in the final analysis.

Mixed effects models were performed for the following biomarkers or FAs ratios: the ratio of DHA: EPA, the ratio of PUFA: SFA, and FA percentage data for diatom biomarkers 16:4n-1 and EPA, and dino+flag biomarkers 18:5n-3 and DHA. We followed the recommendations in Zuur et al. (2009) for fitting FA mixed effects models. First, the optimal

random effect structure (which could be no random effect) was fitted for the full model using restricted maximum likelihood estimation. Second, we used maximum likelihood estimation to determine the most parsimonious fixed effect model structure, with the optimal random structure as determined in step one. Finally, the most parsimonious model for each FA, which included the optimal random and fixed effect structures, was re-fitted with restricted maximum likelihood estimation. Determination of the most parsimonious model in each step was decided using Akaike Information Criterion corrected for small sample sizes (AICc, Burnham and Anderson, 2002). In the instances where more than one model had similar AICc scores (<1 AICc), we chose the model with the lower number of explanatory variables. For simplicity, we report only the final parsimonious model for each FA biomarker in the results.

To predict integrated EPA (mg m^{-2}) concentrations, we fit a mixed effects model to the EPA concentration data. The biological, chemical, and physical survey data was sampled at a higher vertical and spatial sampling resolution (n = 1656) compared to the FA sampling (n=164), thus the model allowed for predicting integrated water column EPA concentrations for all surveyed stations. Predictive models were computed using natural log-transformed data, thus a correction was applied to re-convert predicted EPA concentrations (Duan, 1983).

All analyses were done using R version 3.6 (R Core Team, 2018). Mixed effects models were fitted using the "*nlme*" package (Pinheiro et al., 2017), AICc using the "*AICcmodavg*" package (Mazerolle and Mazerolle, 2019), and type II regressions were computed using the "*smatr*" package (Warton et al., 2012).

3. Results

3.1. Spatial patterns of Chl-a and FA concentrations

Generally, areas of higher-than-average Chl-a were spatially associated with higher total FA concentrations. Average water column (0-50 m) Chl-a measurements were higher in June 2017 and 2018 compared to Aug/Sep 2017 and 2019, though high variability existed among stations and across all surveys (Fig. 1). Elevated water column average Chl-a concentrations (>6 mg m^{-3}) were present north of St. Lawrence Island within and north of the Bering Strait in both June 2017 and 2018, areas that similarly showed elevated (> 15 mg m^{-3}) concentrations of total FAs. Total Chl-a concentrations had highly significant positive correlations with the > 20 μm size-fractioned concentrations (Table S1), indicating that communities were comprised of large phytoplankton in areas with high concentrations of total Chl-a.

3.2. Seasonal dynamics of FA biomarkers

Total FA concentrations (mean ±SD) in June 2017 were significantly higher than all other surveys (average across stations: 28.2±21.1 mg m^{-3}, $p<0.05$, Tukey HSD, Figs. 1, 2A), followed by FA concentrations in June 2018 (22.2 ±16.9 mg m^{-3}), Aug/Sep 2019 (18.8±16.5 mg m^{-3}), and Aug/Sep 2017 (12.1±5.4 mg m^{-3}). Overall SFA, and MUFA concentrations were higher in June compared to Aug/Sep (Fig. 2A), however percent PUFA levels were highest in Aug/Sep 2019 (Fig. 2D). The diatom biomarkers 16:1n-7, 16:4n-1, and EPA all varied significantly among season and year (Tukey HSD, $F(3,163) = 10.6$, 4.2, and 4.3, respectively, $p< 0.05$, Fig.

2B). Concentrations of 16:1n-7 and 16:4n-1 and EPA were significantly higher in June than in Aug/Sep except for EPA, where values in Aug/Sep 2019 were similar to values in June. The diatom biomarkers (percentage of 16:1n-7, 16:4n-1 and EPA, Fig. 2E) showed similar patterns to the concentration data.

The concentration of dino+flag-associated biomarkers 18:5n-3(0.8± 1.0 mg m^{-3}) and DHA (1.5± 1.6 mg m^{-3}) were significantly higher in Aug/Sep 2019 compared to all other surveys (Tukey HSD, $p<0.05$, Fig. 2C). The dino+flag biomarker 18:4n-3 was significantly higher in Aug/Sep 2019 than in Aug/Sep 2017 (Tukey HSD, $p<0.05$), but otherwise showed no difference among seasons and years. The dino+flag percent FA data and the sum of n-3 PUFAs showed overall similar patterns to the concentration data, with Aug/Sep 2019 values being the highest (Fig. 2F). Resultant DHA: EPA ratios were significantly higher in Aug/Sep compared to June (Tukey HSD, $p<0.05$, Fig. 2C). The diatom biomarkers of EPA, 16:1n-7, and 16:4n-1 were all correlated positively for both the concentration (Table S1) and percentage data (Table S2). Similarly, DHA correlated well with the dino+flag biomarkers 18:4n-3 and 18:5n-3 for both the concentration and percentage data (Table S1-S2).

Multivariate nMDS analysis of the FA percentage composition data similarly showed clear differences among seasons and years (Fig. 3). FA biomarkers most responsible for the separation of seasons were diatom biomarkers (i.e. 16:1n-7, 16:2n-4, 16:4n-1 and EPA), which appeared to be more highly associated with the June 2017 and 2018 samples. In contrast, dino+flag markers (i.e. 18:3n-3, 18:4n-3, 18:5n-3, and 22:6n-3) were more closely associated with the Aug/Sep 2017 and 2019 samples. However, substantial variability of the FA compositions in each survey also indicated spatial differences in phytoplankton communities.

3.3. Taxonomic comparison of FA biomarkers and FlowCAM images

FlowCAM-measured diatom and dinoflagellate biovolumes correlated positively with their taxa-associated FA biomarkers. Significant positive correlations were observed between log_{10}-transformed diatom biovolumes and FA concentrations of EPA (Fig. 4A, $r^2 = 0.41$, $p < 0.01$, $df = 38$), 16:1n-7 (Fig. 4C, $r^2 = 0.45$, $p < 0.01$, $df = 38$), and 16:4n-1 (Fig. 4E, $r^2 = 0.46$, $p < 0.01$, $df = 38$) in June 2017 and Aug/Sep 2017. However, when analyzing only the Aug/Sep 2017 diatom data, correlations were not significant ($p > 0.05$, $df = 22$). The lack of correlation, appeared to be driven by samples with low FlowCAM diatom biovolumes that were associated with relatively higher diatom FA biomarker values (Fig 4A, Fig S1), something that occurred when the contribution of diatoms to the total phytoplankton composition (Fig. S1) and abundance were low. These result indicates that when diatoms were low in total abundance, other taxa may have contributed to the FA biomarker pool commonly associated with diatoms (EPA, 16:4n-1, 16:1n-7). In addition, only diatoms >20 µm in length were quantified by FlowCAM analysis, possibly missing smaller diatoms compared to FA samples where all particles captured on 0.7 µm filters were analyzed. Dinoflagellate biovolumes correlated positively with FA concentrations of DHA (Fig. 4B, $r^2 = 0.51$, $p < 0.01$, $df = 20$) and 18:5n-3 (Fig. 4D, $r^2 = 0.55$, $p < 0.01$, $df = 20$) in June 2017. Additionally, the ratio of DHA to EPA correlated positively with the FlowCAM-measured ratio of dinoflagellate to diatom biovolumes (Fig. 4F, $r^2 = 0.45$, $p < 0.01$, $df = 20$) in June 2017.

3.4. Associations between FA biomarkers and environmental conditions

Next, we analyzed associations between the individual environmental variables and the FA concentration and percentage biomarkers using log_{10}-transformed data from discrete samples. Some of the primary pairwise correlations are shown in Figure 5 and highlighted below, while all regressions are presented in Table S1 and Table S2.

Overall, the majority of the individual FAs (mg m^{-3}) correlated positively and significantly with total and size-fractionated (<5 µm, 5-20 µm, >20 µm) Chl-a data (Fig. 5A-F, Table S1). The strongest relationship for total FAs was with total and >20 µm Chl-a concentrations ($r^2 = 0.52$, $p<0.01$), which in turn were highly correlated ($r^2= 0.90$, $p<0.01$) (Fig. 5A, Table S1). Significant correlations were also found for PUFA concentrations, diatom biomarkers 16:1n-7 and EPA with total and >20 µm Chl-a concentrations (Fig. 5B-D, $r^2 = 0.37$ to 0.52, $p<0.01$, Table S1). In contrast, dino+flag biomarkers 18:5n-3, 18:4n-3 and DHA had the highest correlations with small size fractions of Chl-a (< 5 um) ($r^2 = 0.36$ to 0.67, $p<0.01$, Table S1); positive but weaker correlations were also found with total Chl-a (Fig 5.E, $r^2 = 0.05$ to 0.23, $p<0.05$). Nutrients correlated negatively with temperature and positively with salinity (Fig. 5G, Table S1). We found few significant pairwise relationships between FA concentrations and temperature, salinity, and nutrient concentrations and those relationships were weak (Table S1). DHA: EPA ratios were lowest in cold, high salinity waters (Fig. 5H) and correlated negatively with nitrate concentrations (Fig. 5I, $r^2 = 0.31$, $p<0.01$, Table S1).

The percentage FA results suggested that diatoms are higher in relative biomass in colder, high salinity waters and in areas of higher nitrate (Table S2). Percentage of dino+flag FA biomarkers were higher in warmer waters and in areas with low nutrient concentrations (Table S2). Total and large (>20 µm) size-fractioned Chl-a correlated positively with the percentage diatom biomarkers (16:1n-7, 16:4n-1, 16:2n-4, and EPA) but negatively with the percent

contribution of dino+flag-associated FA biomarkers (18:4n-3, 18:5n-3, and DHA) and the ratio of DHA to EPA (Fig. 5F, Table S2). Percentage diatom FA biomarkers associated negatively with the dino+flag and SFA. The percentage contribution from bacterial FA biomarkers correlated positively with the diatom biomarkers, and >20 µm, 5-20 µm, and total Chl-a, but negatively with several dino+flag biomarkers. For both the percentage and concentration data, the patterns observed for all 4 surveys combined were generally also visible within each survey (data not shown).

3.5. FA mixed effects models

Mixed effects models using the FA percentage data showed that several environmental variables influenced FA phytoplankton dynamics. The most parsimonious mixed effects models consistently included survey as a random effect. All statistical values are reported in Table S3; below we report the main findings. Percent EPA contribution correlated positively with total Chl-a concentrations and with vertical depth position (Table S3). EPA values were higher in and below the mixed layer than above the mixed layer; though the effect of vertical position was included in the final model, its influence was minor.

The diatom biomarker 16:4n-1 showed significant positive relationships with total Chl-a and nitrogen concentrations but a negative relationship with temperature. Percent DHA was positively related to total Chl-a, but negatively related to nitrogen concentrations (Table S3). The dino+flag marker 18:5n-3 was negatively related to both total Chl-a and nitrogen concentrations. DHA: EPA ratios were also negatively related to Chl-a and nitrogen concentrations, while

relating positively with salinity and temperature. The ratio of PUFA: SFA increased with Chl-a concentrations, but decreased with nitrogen concentrations and temperature (Table S3).

Lastly, we used a mixed effects model to enable predictions of absolute EPA concentrations (Fig. 6). The most parsimonious model, assessed using AICc, included log-transformed total Chl-a and log-transformed nitrogen (sum of nitrate and ammonium) as the fixed effect and a random structure consisting of an interaction of Chl-a and survey (Table S4). Model prediction of EPA correlated strongly with measured EPA concentrations ($r^2 = 0.63$, $p < 0.01$, df = 151, Fig. S2A). Variability and thus uncertainty of EPA model predictions were highest in samples with total Chl-a concentrations >5 mg m^{-3} (Fig. S2B). Next we calculated water column integrated EPA concentrations using the EPA model fitted with the full environmental dataset (n=1656). Water column integrated EPA concentrations differed significantly among all four surveys (Fig. 6, Tukey HSD, $p<0.05$), with average values highest in June 2018 (93 ± 60 mg m^{-2}), followed by June 2017 (66 ± 46 mg m^{-2}), Aug/Sep 2019 (54 ± 30 mg m^{-2}), and Aug/Sep 2017 (30 ± 8 mg m^{-2}). Throughout, there was high spatial variation in the predictions with the highest concentrations reaching levels of 264 mg m^{-2} and 241 mg m^{-2} in June 2017 and 2018, while highest values in Aug/Sep 2017 were 54 mg m^{-2} and 198 mg m^{-2} in Aug/Sep 2019.

4. Discussion

Seston FA biomarkers reflected phytoplankton community shifts from diatoms dominating in spring followed by late summer increases of dinoflagellates and small flagellates.

High total FA and PUFA concentrations in late spring (June) primarily synthesized by diatoms suggest that phytoplankton FAs from this time period provide important high quality dietary subsidies for consumers (Grebmeier et al., 2006). Diatom and dinoflagellate biovolume measurements from FlowCAM images in general correlated positively with their respective FA biomarkers, confirming that FA compositional data can provide reliable information on phytoplankton community dynamics. However, our analyses also showed one exception to that pattern. The correlations between diatom FA biomarkers and diatom flowCAM data were insignificant during Aug/Sep 2017, highlighting taxonomic identification from FA field samples can be limited when the contribution of a specific taxonomic group to the total phytoplankton pool is very low. Measured phytoplankton FA composition (concentrations and percentages) varied with changes in temperature and nitrogen, likely due to a combination of species-specific physiological responses as well as changes in the phytoplankton community species composition (Grosse et al., 2019; Jiang and Gao, 2004). Lastly, derived EPA concentrations from a model that used commonly sampled survey data (e.g., temperature, nitrogen, and Chl-a) demonstrated broad-scale water column estimates of dietary EPA available to consumers at the base of the northern Bering and Chukchi Sea food webs.

4.1. FA biomarker and FlowCAM estimates of diatoms and dinoflagellates

Taxonomic information from microscopy imaging techniques generally confirmed that observed FA biomarker patterns can be associated with dominant phytoplankton taxa groups. Although FlowCAM-measured diatom and dinoflagellate biovolumes correlated positively with diatom and dinoflagellate FA biomarker concentrations, these data also revealed substantial

unexplained variance. The combined June and Aug/Sep 2017 data yielded significant trends for diatom biovolumes and their FA biomarkers (16:1n-7, 16:4n-1 and EPA) however, similar diatom trends were insignificant when using only samples from Aug/Sep 2017. During Aug/Sep 2017 when diatoms constituted a low contribution to the total phytoplankton composition, and overall total Chl-a concentrations were also low, our results showed that FA diatom biomarkers were relatively higher compared to diatom biovolumes estimates from FlowCAM. We speculate that in these instances we either undercounted small diatoms (below our FlowCAM < 20 µm length threshold) or FA contributions from other groups contributed to the FA pools of the diatom associated biomarkers. For example, *Synechococcus* (a pico-cyanobacteria), which can contain 16:1n-7 (Jónasdóttir, 2019), were observed as up to 20% of the phytoplankton carbon biomass in some areas during Aug/Sep 2017 (data not shown). Similarly, contribution to the diatom associated FA pool could have come from chlorophytes containing 16:4n-1, chlorophytes and cryptophytes containing EPA (Jónasdóttir, 2019), or from protozoans, including ciliates, which are known to contain substantial amounts of EPA (Dutz and Peters, 2008).

Differentiating between dinoflagellates, heterotrophic flagellates and flagellates using FA biomarkers alone is challenging. The observable trends between 18:5n-3 and DHA with dinoflagellate identified from the FlowCAM suggest that noticeable FA contributions at least partially originated from dinoflagellates, however, small flagellates, not measured with the FlowCAM analysis, may also be important. Dinoflagellate and small flagellates often co-occur. Higher percentages of 18:1n-9 and 18:0 in some Aug/Sep 2017 samples could indicate increased contributions from smaller flagellates (Reuss and Poulsen, 2002), but these quite ubiquitous FAs are also present in several other taxa (Cañavate, 2019). The significant association between dinoflagellate biovolumes and their specific FA biomarkers (DHA, 18:5n-3) differ from a recent

study by Marmillot et al. (2020) from the Canadian Arctic, which found no significant relationships for dinoflagellates. We speculate that these differences may be explained by the fact that flagellates are a diverse group of organisms including autotrophic, mixotrophic (i.e., organisms being both autotrophic and heterotrophic) and heterotrophic species, which can vary substantially in FA signatures depending on their diet intake, ability to retain specific compounds, and responses to environmental conditions. Overall, our results are in agreement with previous field studies (Marmillot et al., 2020; Reuss and Poulsen, 2002; Sushchik et al., 2004), and highlights the utility of FA biomarkers for depicting relative contributions of major phytoplankton taxonomic groups, except when a specific taxa constitutes only a minor percentage of the total phytoplankton composition.

4.2. Factors influencing seston FA dynamics

Seasonal shifts were clearly visible in the FA biomarkers, with highest abundances of diatom FAs in spring followed by increasing dino+flag FAs in late summer. These seasonal shifts agree well with phytoplankton taxonomic analysis from the northern Bering and Chukchi seas (Laney and Sosik, 2014; Lee et al., 2019; Sukhanova et al., 2009) and with FA biomarker studies in other Arctic regions (Connelly et al., 2016; Falk-Petersen et al., 1998). Chl-a concentration was the primary predictor variable for almost all FA biomarker concentrations. These linkages were particularly strong between absolute concentrations of the diatom biomarkers, 16:4n-1, 16:1n-7 and EPA, and the total and the large (>20 μm) size fraction Chl-a. The high positive correlation of the >20 μm fraction with total Chl-a suggests that large phytoplankton primarily of diatom origin were driving changes in total Chl-a concentrations.

Shifting environmental conditions influence seston FA dynamics through both individual phytoplankton species and community composition responses (Cañavate et al., 2019; Miller et al., 2017). Temperature and nitrogen (nitrate + ammonium) concentrations influenced the percentage FA patterns. Temperature correlated negatively with the ratio of PUFAs to SFAs, a pattern that is likely driven by decreasing PUFA concentrations with warming (Hixson and Arts, 2016; Jiang and Gao, 2004). Relative concentration of dino+flag biomarkers increased with decreasing nitrogen concentrations, warmer temperatures and lower salinity, supporting the premise that dinoflagellates and small flagellates are commonly more prevalent in low nutrient environments, as previously observed during summer in the eastern Bering Sea (Moran et al., 2012; Sukhanova et al., 2009). Differences in residual nutrient concentrations among water masses are associated with different phytoplankton communities (Danielson et al., 2017), which also likely explain the higher percentages of FA diatom biomarkers in colder, more saline, nutrient-rich waters. Differences in FA compositions with depth, as shown using the mixed effects modeling, for example for percentages of EPA, also indicate that diatoms are more prevalent in deeper, higher nutrient waters near the subsurface Chl-a maximum, a common summer feature in arctic shelf ecosystems (Lowry et al., 2015; Martini et al., 2016). In contrast, higher abundance of FA dino+flag biomarkers tend to occur closer to the surface in waters with lower nutrient concentrations, where they may have an advantage compared to, for example, diatoms. Higher surface area to volume ratios of small flagellates allow enhanced access to nutrients at low concentrations (Edwards et al., 2012), while many dinoflagellates maintain higher growth by migrating daily from deeper, nutrient rich water to the surface (Jephson and Carlsson, 2009) and also engage in heterotropy. Though the environmentally linked FA biomarker compositional shifts were likely due to community level responses, changes at the

individual species level also occur. For example, increasing temperatures and nitrogen limitation at the individual species level can both result in increasing SFAs and MUFAs, and contrarily in decreasing PUFA levels (de Jesús-Campos et al., 2020). However, species responses to both temperature and nutrient limitation differ among algae (Bi et al., 2014) and also change with evolutionary responses (O'Donnell et al., 2019).

4.3. Importance of dietary FAs for consumers

Variation in plankton communities and their nutritional quality (i.e. lipid and essential FAs) influence spatiotemporal trends in food quality available to consumers (Twining et al., 2016). The availability of essential EPA strongly influences growth of copepod nauplii (Leiknes et al., 2016), fish (Copeman and Laurel, 2010; Copeman et al., 2022), juvenile crab (Copeman et al. 2021) and benthic organisms (Schollmeier et al., 2018), as well as overall ecosystem production (Litzow et al., 2006). Using the full survey data, we calculated water column integrated EPA concentrations over a survey-wide spatial scale. Overall, the modeled EPA predictions compared well to measured EPA concentrations. Modeled EPA data may provide a first step towards a broader characterization of dietary availability of essential FAs throughout these ecosystems. Overall, predicted EPA concentrations were highest in spring with lower concentrations in late summer, particularly Aug/Sep 2017. The mixed effects model analyses also show that FA spatial predictions vary between seasons and years, as “survey” was a significant explanatory variable in the model. Survey should be considered a proxy for seasonal and interannual changes in the FA pools associated with the phytoplankton community composition. Thus, predictive power increases when accounting for inter- and intra-annual

differences in FA composition patterns, and best results are retrieved if model predictions are coupled with a smaller subset of FA phytoplankton information from the specific year in question. Additional improvements of the current model framework would be inclusion of data from colder years that may have noticeably different phytoplankton communities (Hill et al., 2005) compared to the years 2017-2019, and laboratory studies of regional zooplankton or benthic invertebrate (e.g. crabs, Copeman et al., 2021) growth and reproduction rate responses to dietary availability of essential EPA.

An expected future consequence of warming and increased stratification, including in Arctic regions, is a shift in phytoplankton community structure towards smaller sized cells (Morán et al., 2010) and a prospective decrease in PUFA concentrations (Hixson and Arts, 2016). Such shifts in FA compositions are due to a combination of direct physiological effects on phytoplankton FA synthesis as well as due to phytoplankton community shifts. How changing sea-ice phenology and the resulting effects on ice-associated phytoplankton (Clement Kinney et al., 2020), and spring and summer open water blooms (Song et al., 2021) influences the availability of carbon and thus important dietary FA in the northern Bering and Chukchi Sea ecosystems, remains an open question. Our analyses and model framework provide new regional baseline information on seasonal and inter-annual variation of phytoplankton FAs. Such information will increase the ability to evaluate the impacts of changing environmental conditions and thus dietary lipid on higher trophic level consumers at broader spatial scales.

Declaration of Competing Interest

The authors declare no known competing financial interests or personal relationships that could have appeared to influence the work reported in this manuscript.

Acknowledgements

We are grateful to Brendan Smith, Miranda Irby, Ed Farley, Anna Mounsey, Haley Cynar, Jeff Krause, Harmony Wayner, and Steven Baer for help during field sampling, Peter Proctor and Eric Wisegarver for analysis of the nutrient data, and the crews of the *R/V's Ocean Star* and *Sikuliaq*. We are thankful to Lauren Rogers for help with mixed effects models, and comments from Jeanette Gann, Fletcher Sewall, and two anonymous reviewers that substantially helped improve the manuscript. We thank Carlissa Salant, Michelle Stowell, and Jami Ivory for general analytical assistance in the Marine Lipid Ecology Lab in Newport, OR, and the funding sources: NPRB Arctic IERP (Arctic IES LTL (A92), ASGARD, Phytoplankton Gap proposal (A96), and National Science Foundation Office of Polar Programs award numbers OCE-1603460 (ML). The findings and conclusions in this paper are those of the authors and do not necessarily represent the views of the National Marine Fisheries Service, NOAA. Reference to trade names does not imply endorsement by the National Marine Fisheries Service, NOAA. This manuscript is a product of the North Pacific Research Board Arctic Integrated Ecosystem Research Program [https://www.nprb.org/arctic-program] NPRB publication number ArcticIERP-25. This is EcoFOCI contribution number EcoFOCI-1005 and PMEL contribution number 5325. This publication was partially funded by the Cooperative Institute for Climate, Ocean, & Ecosystem

Studies (CIOCES) under NOAA Cooperative Agreement NA20OAR4320271, Contribution No 2021-1168.

References

Álvarez, E., Moyano, M., López-Urrutia, Á., Nogueira, E., Scharek, R., 2014. Routine determination of plankton community composition and size structure: a comparison between FlowCAM and light microscopy. Journal of plankton research 36, 170-184.

Baker, M.R., Farley, E.V., Ladd, C., Danielson, S.L., Stafford, K.M., Huntington, H.P., Dickson, D.M., 2020. Integrated ecosystem research in the Pacific Arctic–understanding ecosystem processes timing and change. Deep-Sea Res. II 177, 104850. https://doi.org/10.1016/j.dsr2.2020.104850

Baker, M.R., Farley, E.V., Danielson, S.L., Mordy, C., Stafford, K.M., Dickson, D.M.S., 2022. Integrated Research in the Arctic – ecosystem linkages and shifts in the northern Bering Sea and eastern and western Chukchi Sea. Deep-Sea Research II. This Issue.

Bell, M.V., Batty, R.S., Dick, J.R., Fretwell, K., Navarro, J.C., Sargent, J.R., 1995. Dietary deficiency of docosahexaenoic acid impairs vision at low light intensities in juvenile herring (Clupea harengus L.). Lipids 30, 443.

Bell, M.V., Tocher, D.R., 2009. Biosynthesis of polyunsaturated fatty acids in aquatic ecosystems: general pathways and new directions, Lipids in aquatic ecosystems. Springer, pp. 211-236.

Bi, R., Arndt, C., Sommer, U., 2014. Linking elements to biochemicals: effects of nutrient supply ratios and growth rates on fatty acid composition of phytoplankton species. Journal of Phycology 50, 117-130.

Budge, S.M., Devred, E., Forget, M.-H., Stuart, V., Trzcinski, M.K., Sathyendranath, S., Platt, T., 2014. Estimating concentrations of essential omega-3 fatty acids in the ocean: supply and demand. ICES Journal of Marine Science 71, 1885-1893.

Budge, S.M., Iverson, S.J., Koopman, H.N., 2006. Studying trophic ecology in marine ecosystems using fatty acids: a primer on analysis and interpretation. Marine Mammal Science 22, 759-801.

Budge, S.M., Parrish, C.C., 1998. Lipid biogeochemistry of plankton, settling matter and sediments in Trinity Bay, Newfoundland. II. Fatty acids. Organic Geochemistry 29, 1547-1559.

Burnham, K., Anderson, D., 2002. Model selection and multimodel inference: a practical information-theoretic approach. The University of Chicago Press New York.

Cañavate, J.-P., van Bergeijk, S., Giráldez, I., González-Ortegón, E., Vílas, C., 2019. Fatty Acids to Quantify Phytoplankton Functional Groups and Their Spatiotemporal Dynamics in a Highly Turbid Estuary. Estuaries and Coasts 42, 1971-1990.

Cañavate, J.P., 2019. Advancing assessment of marine phytoplankton community structure and nutritional value from fatty acid profiles of cultured microalgae. Reviews in Aquaculture 11, 527-549.

Clement Kinney, J., Maslowski, W., Osinski, R., Jin, M., Frants, M., Jeffery, N., Lee, Y.J., 2020. Hidden production: on the importance of pelagic phytoplankton blooms beneath Arctic Sea ice. Journal of Geophysical Research: Oceans 125, e2020JC016211.
Connelly, T.L., Businski, T.N., Deibel, D., Parrish, C.C., Trela, P., 2016. Annual cycle and spatial trends in fatty acid composition of suspended particulate organic matter across the Beaufort Sea shelf. Estuarine, Coastal and Shelf Science 181, 170-181.
Copeman, L., Laurel, B., 2010. Experimental evidence of fatty acid limited growth and survival in Pacific cod larvae. Marine Ecology Progress Series 412, 259-272.
Copeman, L.A., Salant, C.D., Stowell, M.A., Spencer, M.L., Kimmel, D.G., Pinchuk, A.I., Laurel, B.J., 2022. Annual and spatial variation in the condition and lipid storage of juvenile Chukchi Sea gadids during a recent period of environmental warming (2012–2019). Deep Sea Research Part II: Topical Studies in Oceanography, 105177.
Dalsgaard, J., John, M.S., Kattner, G., Müller-Navarra, D., Hagen, W., 2003. Fatty acid trophic markers in the pelagic marine environment.
Danielson, S.L., Eisner, L., Ladd, C., Mordy, C., Sousa, L., Weingartner, T.J., 2017. A comparison between late summer 2012 and 2013 water masses, macronutrients, and phytoplankton standing crops in the northern Bering and Chukchi Seas. Deep Sea Research Part II: Topical Studies in Oceanography 135, 7-26.
de Jesús-Campos, D., López-Elías, J.A., Medina-Juarez, L.Á., Carvallo-Ruiz, G., Fimbres-Olivarria, D., Hayano-Kanashiro, C., 2020. Chemical composition, fatty acid profile and molecular changes derived from nitrogen stress in the diatom Chaetoceros muelleri. Aquaculture Reports 16, 100281.
Duan, N., 1983. Smearing estimate: a nonparametric retransformation method. Journal of the American Statistical Association 78, 605-610.
Dunstan, G.A., Volkman, J.K., Barrett, S.M., Leroi, J.-M., Jeffrey, S., 1993. Essential polyunsaturated fatty acids from 14 species of diatom (Bacillariophyceae). Phytochemistry 35, 155-161.
Dutz, J., Peters, J., 2008. Importance and nutritional value of large ciliates for the reproduction of Acartia clausi during the post spring-bloom period in the North Sea. Aquatic microbial ecology 50, 261-277.
Edwards, K.F., Thomas, M.K., Klausmeier, C.A., Litchman, E., 2012. Allometric scaling and taxonomic variation in nutrient utilization traits and maximum growth rate of phytoplankton. Limnology and Oceanography 57, 554-566.
Falk-Petersen, S., Sargent, J., Henderson, J., Hegseth, E., Hop, H., Okolodkov, Y., 1998. Lipids and fatty acids in ice algae and phytoplankton from the Marginal Ice Zone in the Barents Sea. Polar Biology 20, 41-47.
Folch, J., Lees, M., Stanley, G.S., 1957. A simple method for the isolation and purification of total lipides from animal tissues. Journal of biological chemistry 226, 497-509.
Fujiwara, A., Hirawake, T., Suzuki, K., Eisner, L., Imai, I., Nishino, S., Kikuchi, T., Saitoh, S.-I., 2016. Influence of timing of sea ice retreat on phytoplankton size during marginal ice zone bloom period on the Chukchi and Bering shelves. Biogeosciences Discussions 13.
Galloway, A.W., Winder, M., 2015. Partitioning the relative importance of phylogeny and environmental conditions on phytoplankton fatty acids. PLoS One 10, e0130053.
Galloway, A.W.E., Budge, S.M., 2020. The critical importance of experimentation in biomarker-based trophic ecology. Philosophical Transactions of the Royal Society B: Biological Sciences 375, 20190638.

Giesbrecht, K., Varela, D., Wiktor, J., Grebmeier, J., Kelly, B., Long, J., 2019. A decade of summertime measurements of phytoplankton biomass, productivity and assemblage composition in the Pacific Arctic Region from 2006 to 2016. Deep Sea Research Part II: Topical Studies in Oceanography 162, 93-113.

Gordon, L.I., Jennings Jr, J.C., Ross, A.A., Krest, J.M., 1993. A suggested protocol for continuous flow automated analysis of seawater nutrients (phosphate, nitrate, nitrite and silicic acid) in the WOCE Hydrographic Program and the Joint Global Ocean Fluxes Study. WOCE hydrographic program office, methods manual WHPO, 1-52.

Grebmeier, J.M., Cooper, L.W., Feder, H.M., Sirenko, B.I., 2006. Ecosystem dynamics of the Pacific-influenced Northern Bering and Chukchi Seas in the Amerasian Arctic. Progress in Oceanography 71, 331-361.

Grosse, J., Brussaard, C., Boschker, H., 2019. Nutrient limitation driven dynamics of amino acids and fatty acids in coastal phytoplankton. Limnology and Oceanography 64, 302-316.

Hama, T., 1999. Fatty acid composition of particulate matter and photosynthetic products in subarctic and subtropical Pacific. Journal of plankton research 21.

Helenius, L., Budge, S., Duerksen, S., Devred, E., Johnson, C.L., 2019. Lipids at the plant–animal interface: a stable isotope labelling method to evaluate the assimilation of essential fatty acids in the marine copepod Calanus finmarchicus. Journal of Plankton Research 41, 909-924.

Helenius, L., Budge, S.M., Nadeau, H., Johnson, C.L., 2020. Ambient temperature and algal prey type affect essential fatty acid incorporation and trophic upgrading in a herbivorous marine copepod. Philosophical Transactions of the Royal Society B: Biological Sciences 375, 20200039.

Hermann, A.J., Gibson, G.A., Cheng, W., Ortiz, I., Aydin, K., Wang, M., Hollowed, A.B., Holsman, K.K., 2019. Projected biophysical conditions of the Bering Sea to 2100 under multiple emission scenarios. ICES Journal of Marine Science 76, 1280-1304.

Hill, V., Ardyna, M., Lee, S.H., Varela, D.E., 2018. Decadal trends in phytoplankton production in the Pacific Arctic Region from 1950 to 2012. Deep Sea Research Part II: Topical Studies in Oceanography 152, 82-94.

Hill, V., Cota, G., Stockwell, D., 2005. Spring and summer phytoplankton communities in the Chukchi and Eastern Beaufort Seas. Deep Sea Research Part II: Topical Studies in Oceanography 52, 3369-3385.

Hixson, S.M., Arts, M.T., 2016. Climate warming is predicted to reduce omega-3, long-chain, polyunsaturated fatty acid production in phytoplankton. Global Change Biology 22, 2744-2755.

Holmes, R.M., Aminot, A., Kérouel, R., Hooker, B.A., Peterson, B.J., 1999. A simple and precise method for measuring ammonium in marine and freshwater ecosystems. Canadian Journal of Fisheries and Aquatic Sciences 56, 1801-1808.

Huntington, H.P., Danielson, S.L., Wiese, F.K., Baker, M., Boveng, P., Citta, J.J., De Robertis, A., Dickson, D.M., Farley, E., George, J.C., 2020. Evidence suggests potential transformation of the Pacific Arctic ecosystem is underway. Nature Climate Change, 1-7.

Jephson, T., Carlsson, P., 2009. Species-and stratification-dependent diel vertical migration behaviour of three dinoflagellate species in a laboratory study. Journal of plankton research 31, 1353-1362.

Jiang, H., Gao, K., 2004. Effects of lowering temperature during culture on the production of polyunsaturated fatty acids in the marine diatom Phaeodactylum tricornutum (bacillariophyceae) 1. Journal of Phycology 40, 651-654.
Jónasdóttir, S.H., 2019. Fatty acid profiles and production in marine phytoplankton. Marine drugs 17, 151.
Kainz, M., Arts, M.T., Mazumder, A., 2004. Essential fatty acids in the planktonic food web and their ecological role for higher trophic levels. Limnology and Oceanography 49, 1784-1793.
Kaneda, T., 1991. Iso-and anteiso-fatty acids in bacteria: biosynthesis, function, and taxonomic significance. Microbiological reviews 55, 288-302.
Laney, S.R., Sosik, H.M., 2014. Phytoplankton assemblage structure in and around a massive under-ice bloom in the Chukchi Sea. Deep Sea Research Part II: Topical Studies in Oceanography 105, 30-41.
Lee, Y., Min, J.-O., Yang, E.J., Cho, K.-H., Jung, J., Park, J., Moon, J.K., Kang, S.-H., 2019. Influence of sea ice concentration on phytoplankton community structure in the Chukchi and East Siberian Seas, Pacific Arctic Ocean. Deep Sea Research Part I: Oceanographic Research Papers 147, 54-64.
Leiknes, Ø., Etter, S.A., Tokle, N.E., Bergvik, M., Vadstein, O., Olsen, Y., 2016. The Effect of Essential Fatty Acids for the Somatic Growth in Nauplii of Calanus finmarchicus. Frontiers in Marine Science 3, 33.
Litzow, M., A. , Bailey, K., M. , Prahl, F., G. , Ron., H., 2006. Climate regime shifts and reorganization of fish communities: the essential fatty acid limitation hypothesis. Marine Ecology Progress Series 315, 1-11.
Lowry, K.E., Pickart, R.S., Mills, M.M., Brown, Z.W., van Dijken, G.L., Bates, N.R., Arrigo, K.R., 2015. The influence of winter water on phytoplankton blooms in the Chukchi Sea. Deep Sea Research Part II: Topical Studies in Oceanography 118, 53-72.
Marmillot, V., Parrish, C.C., Tremblay, J.-É., Gosselin, M., MacKinnon, J.F., 2020. Environmental and Biological Determinants of Algal Lipids in Western Arctic and Subarctic Seas. Frontiers in Environmental Science.
Martini, K.I., Stabeno, P.J., Ladd, C., Winsor, P., Weingartner, T.J., Mordy, C.W., Eisner, L.B., 2016. Dependence of subsurface chlorophyll on seasonal water masses in the Chukchi Sea. Journal of Geophysical Research: Oceans 121, 1755-1770.
Mazerolle, M.J., Mazerolle, M.M.J., 2019. Package 'AICcmodavg'.
Menden-Deuer, S., Lessard, E.J., 2000. Carbon to volume relationships for dinoflagellates, diatoms, and other protist plankton. Limnology and oceanography 45, 569-579.
Miller, J.A., Peterson, W.T., Copeman, L.A., Du, X., Morgan, C.A., Litz, M.N.C., 2017. Temporal variation in the biochemical ecology of lower trophic levels in the Northern California Current. Progress in Oceanography 155, 1-12.
Moran, S., Lomas, M., Kelly, R., Gradinger, R., Iken, K., Mathis, J., 2012. Seasonal succession of net primary productivity, particulate organic carbon export, and autotrophic community composition in the eastern Bering Sea. Deep Sea Research Part II: Topical Studies in Oceanography 65, 84-97.
Morán, X.A.G., LÓPEZ-URRUTIA, Á., CALVO-DÍAZ, A., Li, W.K., 2010. Increasing importance of small phytoplankton in a warmer ocean. Global Change Biology 16, 1137-1144.

O'Donnell, D.R., Du, Z.y., Litchman, E., 2019. Experimental evolution of phytoplankton fatty acid thermal reaction norms. Evolutionary applications 12, 1201-1211.
Parrish, C., Arts, M., Wainman, B., 1999. Lipids in freshwater ecosystems. New York, SpringeraVerlag. pp. 5a 20.
Parrish, C.C., 2013. Lipids in marine ecosystems. ISRN Oceanography 2013.
Parsons, T.R., 1984. A manual of chemical & biological methods for seawater analysis. Elsevier.
Pinheiro, J., Bates, D., DebRoy, S., Sarkar, D., Heisterkamp, S., Van Willigen, B., Maintainer, R., 2017. Package 'nlme'. Linear and nonlinear mixed effects models, version 3.
Pond, D., Harris, R., Head, R., Harbour, D., 1996. Environmental and nutritional factors determining seasonal variability in the fecundity and egg viability of Calanus helgolandicus in coastal waters off Plymouth, UK. Marine Ecology Progress Series 143, 45-63.
R Core Team, 2018. R: A Language and Environment for Statistical Computing, R Foundation for Statistical Computing, Austria, 2015. ISBN 3-900051-07-0: URL http://www. R-project. org.
Reuss, N., Poulsen, L., 2002. Evaluation of fatty acids as biomarkers for a natural plankton community. A field study of a spring bloom and a post-bloom period off West Greenland. Marine Biology 141, 423-434.
Schollmeier, T., Oliveira, A., Wooller, M., Iken, K., 2018. Tracing sea ice algae into various benthic feeding types on the Chukchi Sea shelf. Polar Biology 41, 207-224.
Sigler, M.F., Stabeno, P.J., Eisner, L.B., Napp, J.M., Mueter, F.J., 2014. Spring and fall phytoplankton blooms in a productive subarctic ecosystem, the eastern Bering Sea, during 1995–2011. Deep Sea Research Part II: Topical Studies in Oceanography 109, 71-83.
Song, H., Ji, R., Jin, M., Li, Y., Feng, Z., Varpe, Ø., Davis, C.S., 2021. Strong and regionally distinct links between ice-retreat timing and phytoplankton production in the Arctic Ocean. Limnology and Oceanography.
Sukhanova, I.N., Flint, M.V., Pautova, L.A., Stockwell, D.A., Grebmeier, J.M., Sergeeva, V.M., 2009. Phytoplankton of the western Arctic in the spring and summer of 2002: Structure and seasonal changes. Deep Sea Research Part II: Topical Studies in Oceanography 56, 1223-1236.
Sushchik, N.N., Gladyshev, M.I., Makhutova, O.N., Kalachova, G.S., Kravchuk, E.S., Ivanova, E.A., 2004. Associating particulate essential fatty acids of the ω3 family with phytoplankton species composition in a Siberian reservoir. Freshwater Biology 49, 1206-1219.
Tocher, D.R., Betancor, M.B., Sprague, M., Olsen, R.E., Napier, J.A., 2019. Omega-3 long-chain polyunsaturated fatty acids, EPA and DHA: bridging the gap between supply and demand. Nutrients 11, 89.
Twining, C.W., Brenna, J.T., Hairston Jr, N.G., Flecker, A.S., 2016. Highly unsaturated fatty acids in nature: what we know and what we need to learn. Oikos 125, 749-760.
Warton, D.I., Duursma, R.A., Falster, D.S., Taskinen, S., 2012. smatr 3–an R package for estimation and inference about allometric lines. Methods in Ecology and Evolution 3, 257-259.
Wasta, Z., Mjøs, S.A., 2013. A database of chromatographic properties and mass spectra of fatty acid methyl esters from omega-3 products. Journal of Chromatography A 1299, 94-102.
Zuur, A., Ieno, E.N., Walker, N., Saveliev, A.A., Smith, G.M., 2009. Mixed effects models and extensions in ecology with R. Springer Science & Business Media.

FIGURES

Figure 1

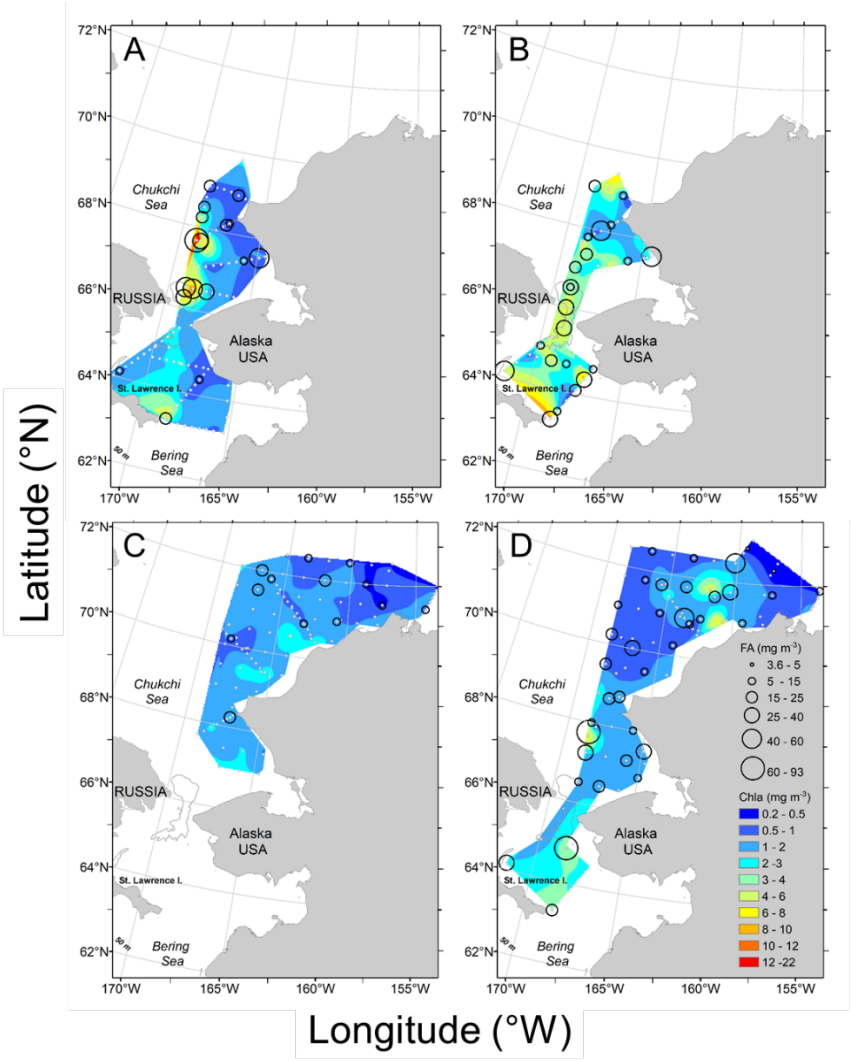

Fig. 1. Mean *in situ* Chl-a [mg m^{-3}] averaged from surface to 50 m and mean total FA concentrations [mg m^{-3}] measured at each station in: **A**) June 2017, **B**) June 2018, **C**) Aug/Sep 2017 and **D**) Aug/Sep 2019 in the northern Bering and Chukchi seas. White diamonds indicate station locations.

Figure 2

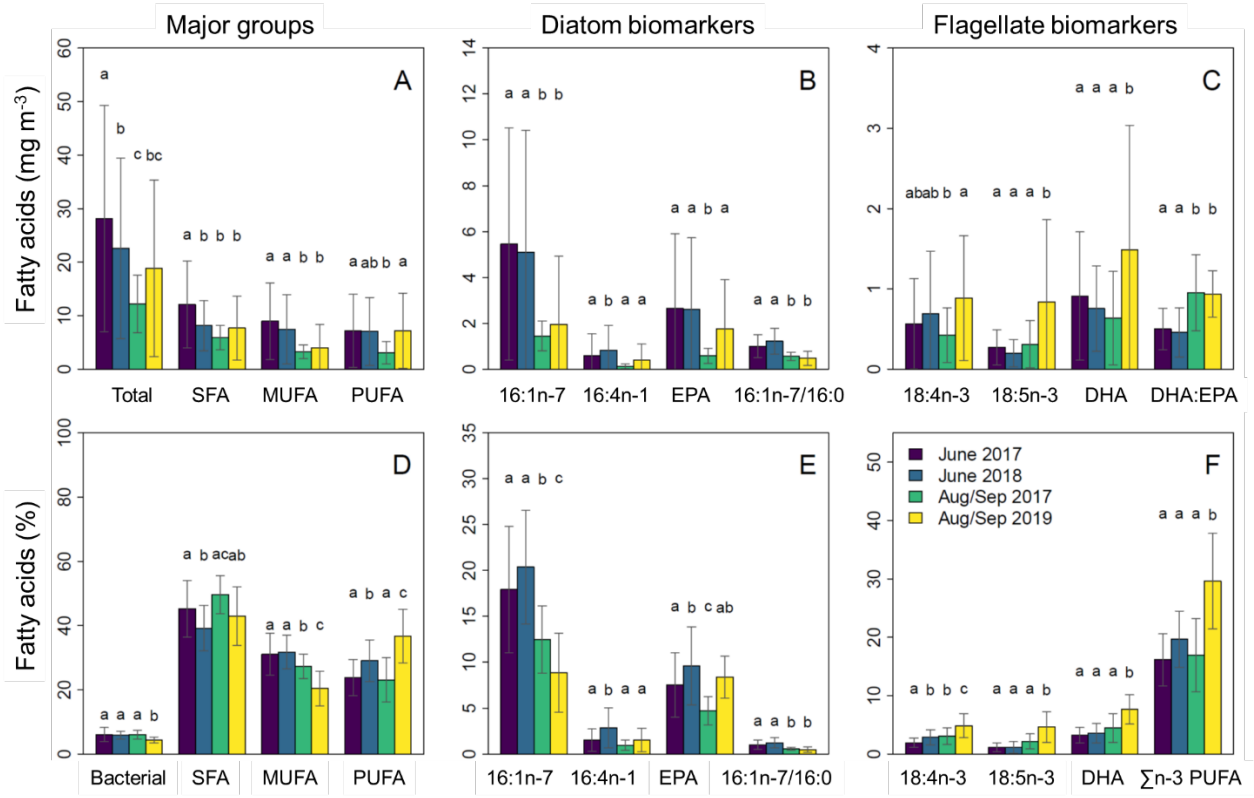

Fig. 2. Differences in June 2017 (n = 42, purple), June 2018 (n = 36, blue), Aug/Sep 2017 (n = 25, green) and Aug/Sep 2019 (n = 61, yellow) FA concentrations (top panel) and percent composition (bottom panel) for total FA, SFA, MUFA, PUFA and Bacterial (sum of all odd carbon FA and branched FAs) (**A, D**), diatom biomarkers 16:1n-7, 16:4n-1 EPA (20:5n-3) and a ratio diatom biomarker (ratio of 16:1n-7/16:0) **(B, E)**, and common dino+flag biomarkers 18:4n-3, 18:5n-3 and DHA (22:6n-3), DHA:EPA ratios, and the sum of n3-PUFA (**C, F**). Letters (a, b, c) denote significant group differences based on ANOVA with Tukey HSD ($p<0.05$), with bars showing mean values and error bars denoting standard deviation.

Figure 3

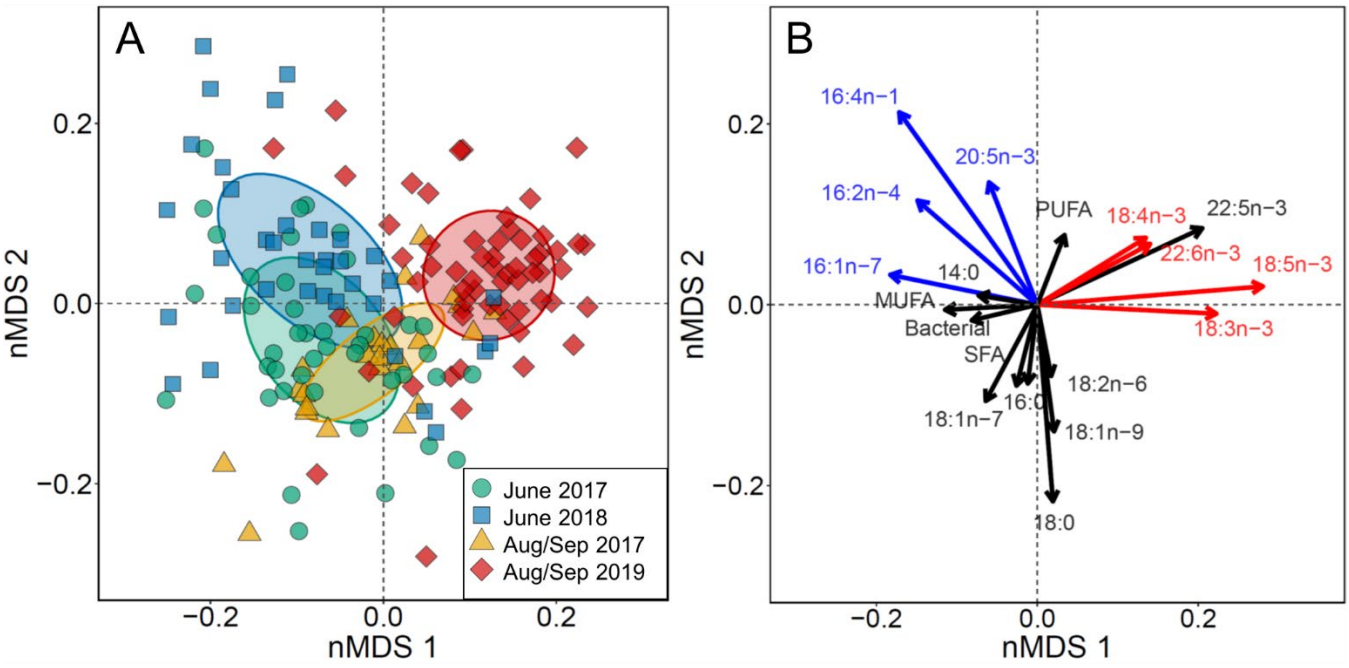

Fig. 3. Non-metric multidimensional scaling (nMDS) of FA percent composition data from each survey, **A**) samples from June 2017 (n = 42, green), June 2018 (n = 36, blue), Aug/Sep 2017 (n = 25, orange) and Aug/Sep 2019 (n = 61, red). Circles denote 50% ellipsoids for each survey. **B**) Vector plot for the nMDS showing individual FAs associated with diatoms (blue), dino+flag (red) and shown in black are all non-taxa specific individual FAs and major FA biomarker groups (SFA, MUFA, PUFA and bacterial).

Figure 4

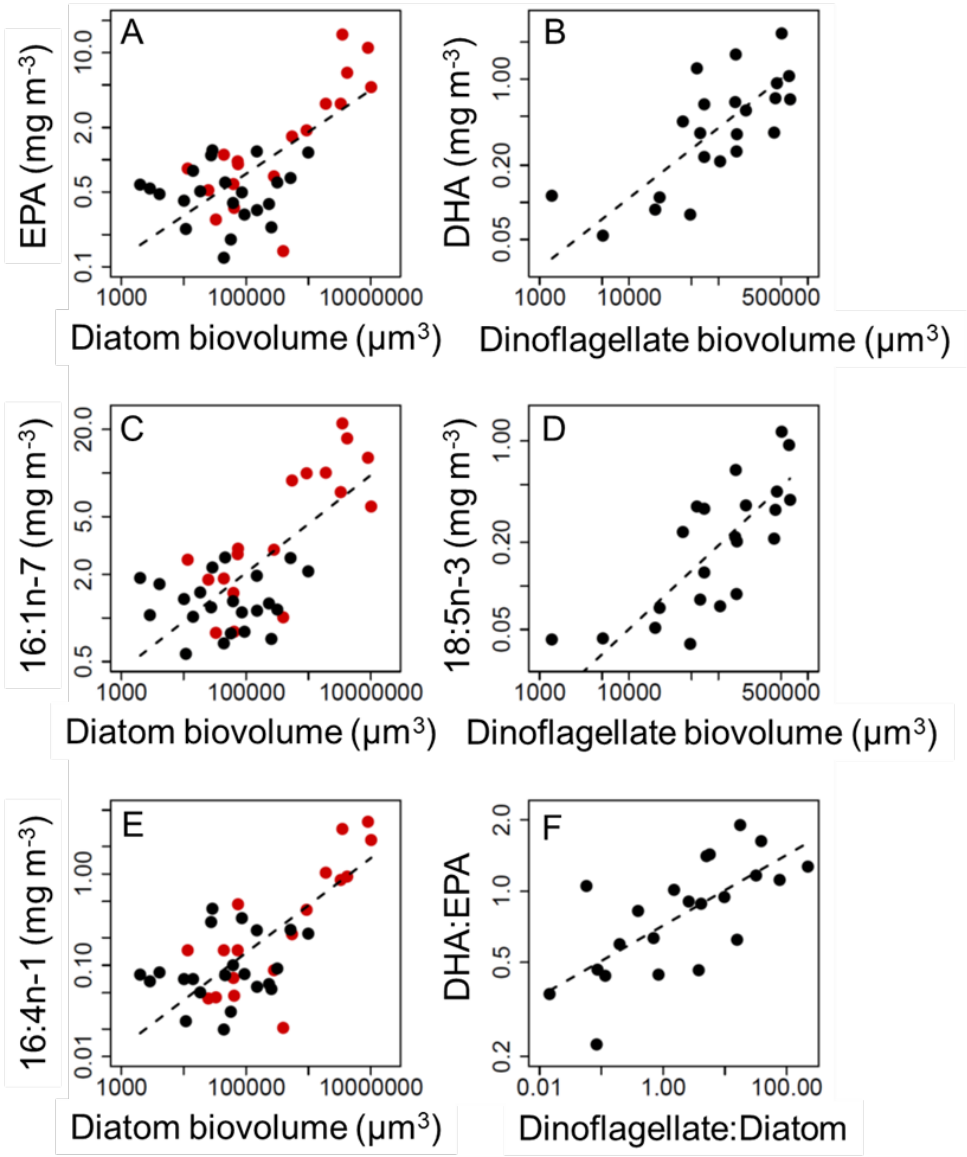

Fig. 4. Comparison of $\log_{10}$ transformed FlowCAM-measured biovolumes and FA biomarker concentrations for diatoms in June 2017 (red, n = 18) and diatoms and dinoflagellates in Aug/Sep 2017 (black, n = 22). Comparisons of diatom biovolumes and **A**) EPA, **C**) 16:1n-7, **E**) 16:4n-1; comparison of dinoflagellate biovolumes and **B**) DHA, **E**) 18:5n-3; and **F**) ratios of dinoflagellate to diatom biovolumes compared to the DHA: EPA biomarkers.

Figure 5

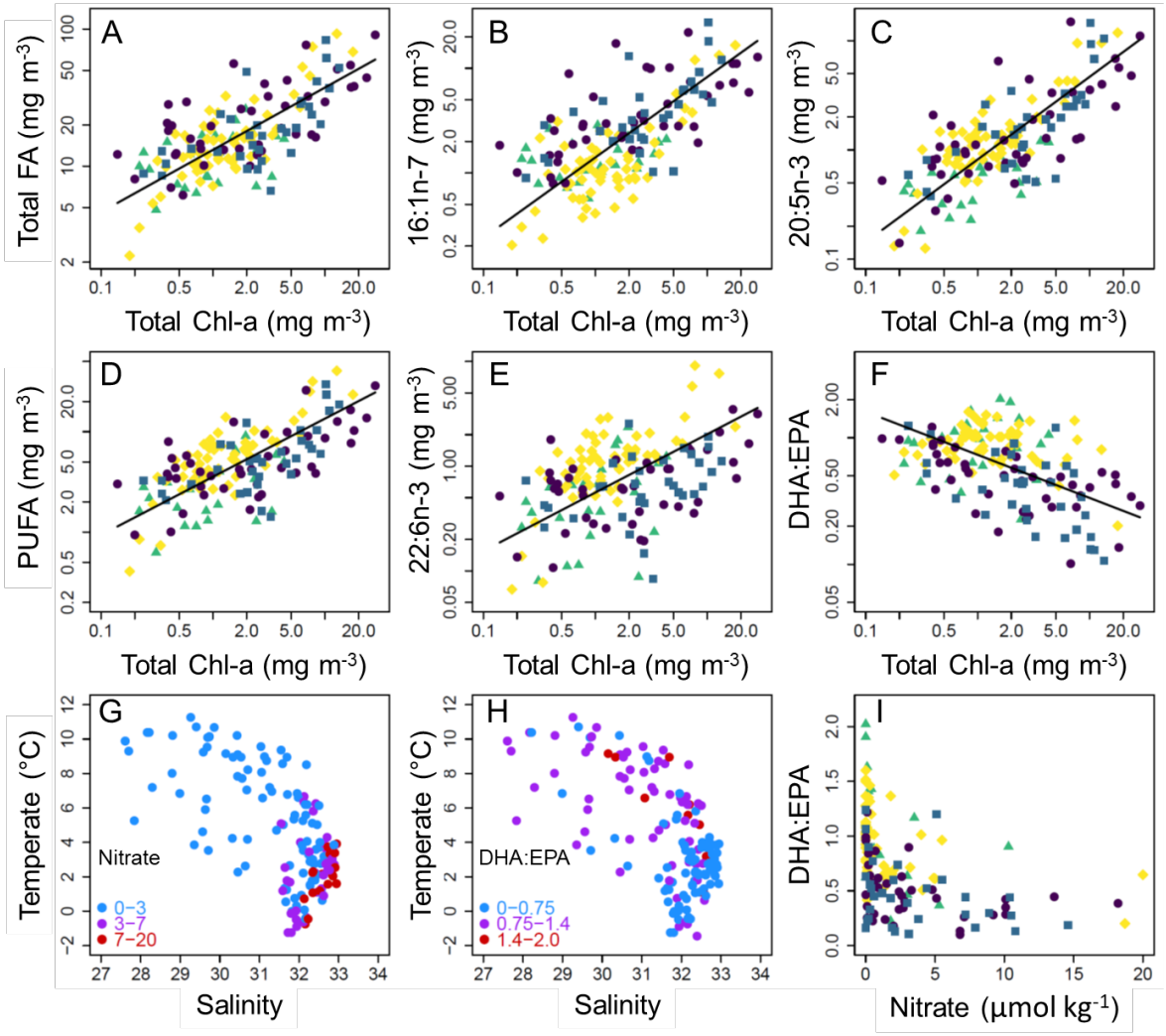

Fig. 5. Selected pairwise Type II regressions using $\log_{10}$-transformed data between *in situ* discrete Chl-a [mg m^{-3}] and FA [mg m^{-3}] samples for **A**) total FAs, **B**) 16:1n-7, **C**) EPA, **D**) total PUFA, **E**) DHA, and **F**) DHA:EPA ratio. Temperature-salinity plots showing **G**) nitrate concentration (µmol kg^{-1}) and **H**) DHA: EPA ratios, color coded by their values (blue=low, red=high), and I) nitrate to DHA: EPA ratios. Colors in plots **A-F** and **I** denote each survey, with June 2017 (purple circles), June 2018 (blue squares), Aug/Sep 2017 (green triangles) and Aug/Sep 2019 (yellow diamonds).

Figure 6

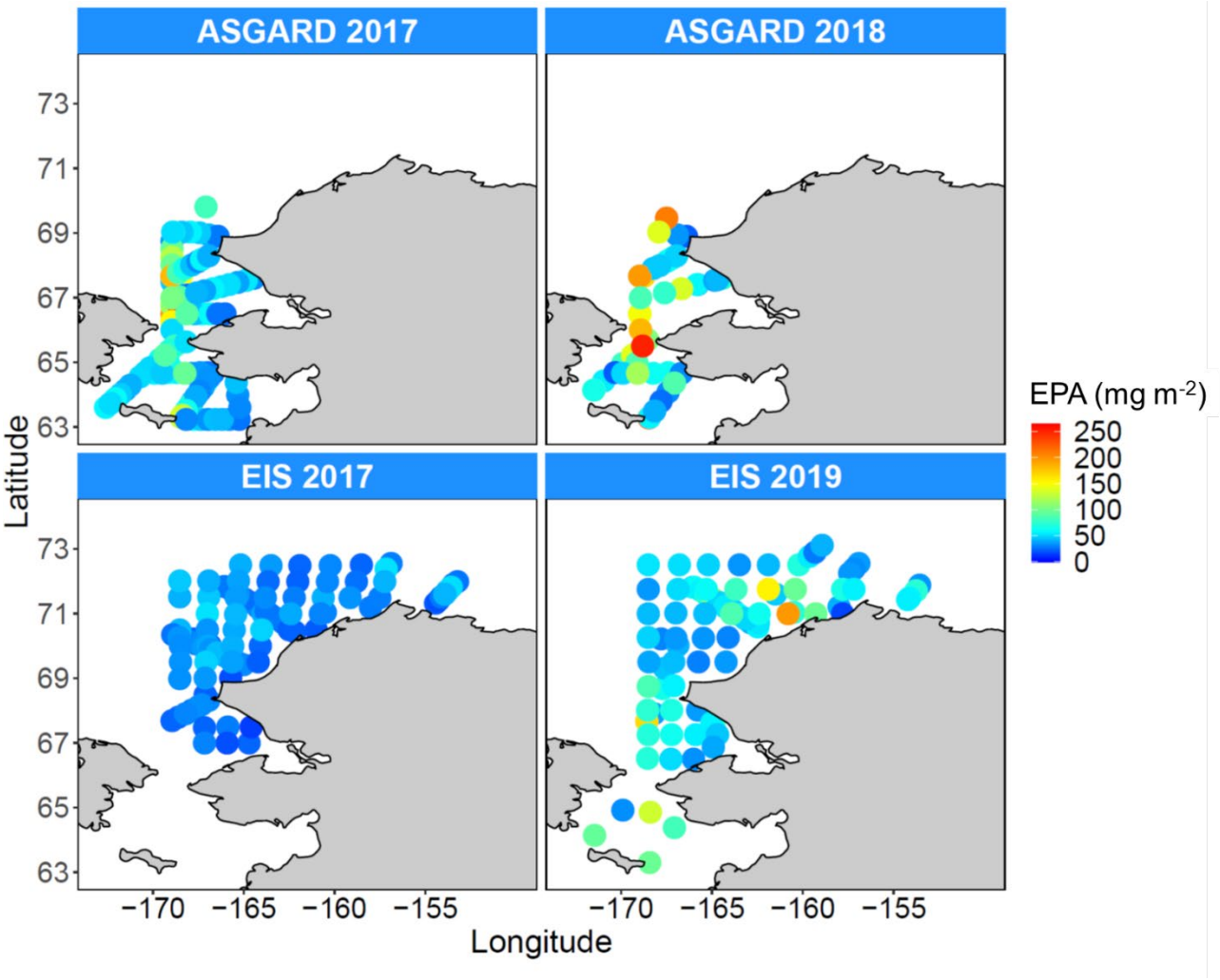

Fig. 6. Mixed effects model results predicting water column integrated EPA concentrations (mg m^{-2}) for each survey using all available discrete total Chl-a and nitrogen samples as predictor variables (n = 1656, Table S2).